Journal of Power Sources 630 (2025) 236046

Contents lists available at ScienceDirect

Journal of Power Sources

journal homepage: www.elsevier.com/locate/jpowsour

Design of functional electrolytes using triple-bonded formate esters as SEI forming additives in graphite anodes

Koji Abe [a,b,*], Masaki Deguchi [a,c], Yanko Marinov Todorov [b]

[a] Graduate School of Sciences and Technology for Innovation, Yamaguchi University, 2-16-1 Tokiwadai, Ube, Yamaguchi, 755-8611, Japan
[b] Organization for Research Initiatives, Yamaguchi University, 2-16-1 Tokiwadai, Ube, Yamaguchi, 755-8611, Japan
[c] Panasonic Energy Co., Ltd., 1-1 Matsushita-cho, Moriguchi, Osaka, 570-8511, Japan

HIGHLIGHTS

- Cyanomethyl formate (CMF) is a new SEI-forming additive for graphite anodes.
- CMF has a higher reductive and oxidative decomposition potentials than VC.
- CMF has low molecular weight, thin SEI, and low cell impedance.
- CMF does not easily cause Al corrosion.

ARTICLE INFO

Keywords:
Electrolyte
Additive
Solid electrolyte interphase
Triple bond
Formate ester

ABSTRACT

The concept of functional electrolytes, in which small amounts of additives are added to the electrolyte to improve the performance of lithium-ion batteries (LIBs), is widely used around the world. Our laboratory has been researching the use of carbonates and sulfonate esters containing triple bonds as additives for solid electrolyte interphase (SEI) formation in anodes and for suppressing the corrosion of Al current collectors. In contrast, formate esters are generally thought to be susceptible to oxidative and reductive decomposition and corrosion. In this work, we attempted to introduce a triple bond into the formate ester, which has currently not received much attention. As a result, we found that the formate ester with a cyanomethyl ($-CH_2C{\equiv}N$) group exhibits excellent cycling performance when added in very small amounts.

1. Introduction

In recent years, the use of lithium-ion batteries (LIBs) has expanded not only as a power source for portable devices, such as notebook PCs, smart phones, and tablets, but also for power systems, such as electric vehicles (EVs, PHVs, HEVs), energy storage systems (ESS), and power tools. The most important features of the LIB are voltages above 4 V and a high energy density, in which the challenge for the electrolyte is how to control the solid electrolyte interphase (SEI) of the graphite anode to reduce decomposition of the main solvent.

The basic concept of the SEI was proposed by E. Peled et al. [1–3]. In 1991, after the Sony Corporation batteries were introduced into the market, the group of D. Auerbach et al. investigated the correlation between the electrochemical properties of Li carbon intercalation electrodes and their surface chemistry in solution. They stated that understanding the surface chemistry of the electrode would enable proper optimization of the electrolyte [4]. Also, the group of J. O. Besenhard and M. Winter et al. stated that the carbon anode requires "filming" of the electrode by electronically insulating permselective "solid electrolyte membranes" being permeable to Li cations but impermeable to any electrolyte component [5]. In this era, the cause of battery performance degradation was the gradual accumulation of unintended electrolyte-derived carbonate and trace impurities in the graphite anode as the number of cycles increased, thus leading to an increased impedance.

At the time, it was believed that propylene carbonate (PC) solvents would cause co-intercalation during lithium insertion into graphite, leading to exfoliation of the graphite and resulting in no battery capacity being achieved. Therefore, commercial electrolytes used in lithium-ion batteries with graphite electrodes were limited to ethylene carbonate

* Corresponding author. Graduate School of Sciences and Technology for Innovation, Yamaguchi University, 2-16-1 Tokiwadai, Ube, Yamaguchi, 755-8611, Japan.
E-mail address: abekoji@yamaguchi-u.ac.jp (K. Abe).

https://doi.org/10.1016/j.jpowsour.2024.236046
Received 22 August 2024; Received in revised form 6 December 2024; Accepted 8 December 2024
Available online 19 December 2024

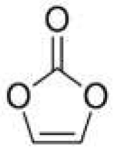

(1a) Vinylene carbonate (VC, MW:86)

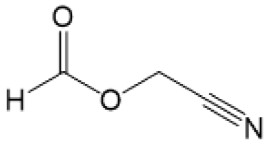

(1b) Cyanomethyl formate (CMF, MW:85)

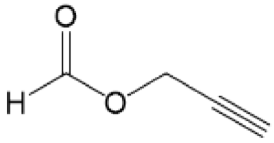

(1c) Propargyl formate (PrF, MW:84)

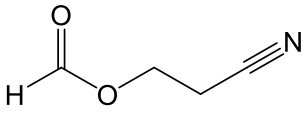

(1d) 2-Cyanoethyl formate (2CEF, MW:99)

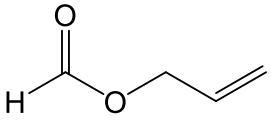

(1e) Allyl formate (AlF, MW:86)

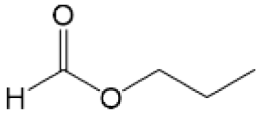

(1f) n-Propyl formate (nPF, MW:88)

Fig. 1. Structures of the additives used in this reaserch.

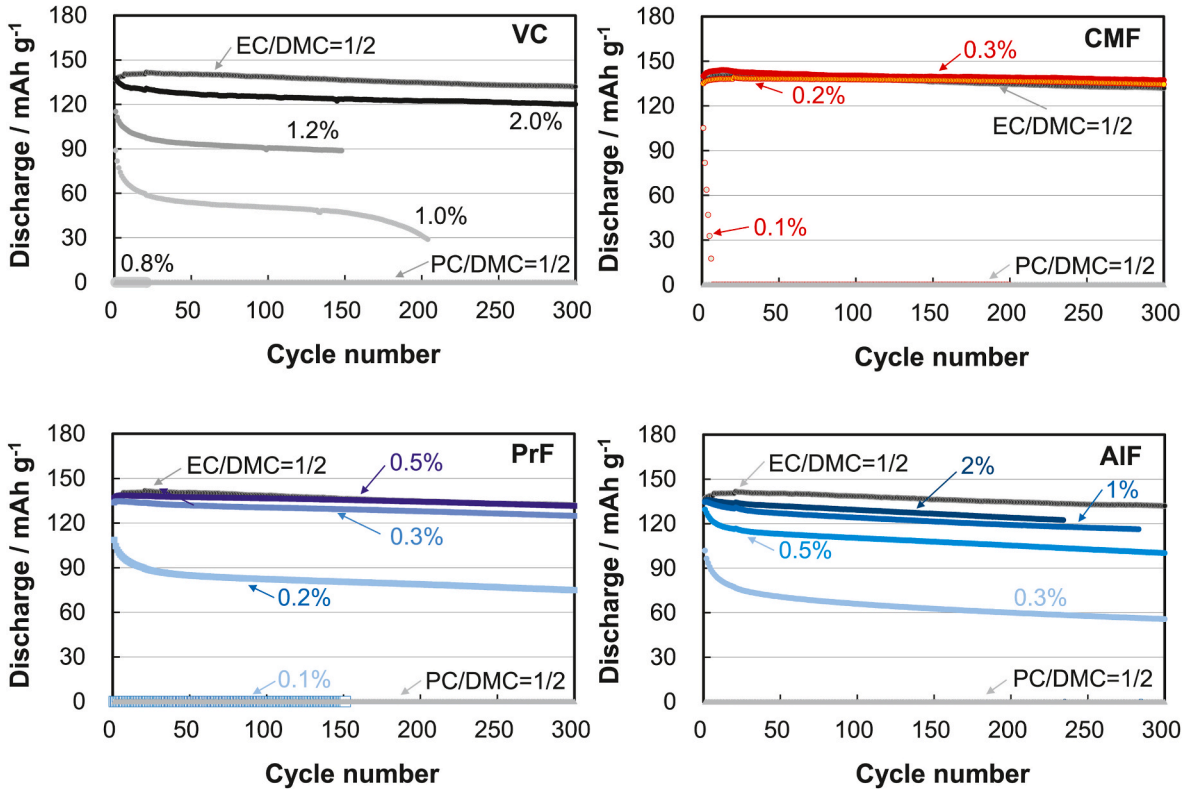

Fig. 2. NCM523/NG full-cell 1C rate cycling performance with 1M $LiPF_6$ PC/DMC = 1/2 (v/v) + additive, reference is 1M $LiPF_6$ EC/DMC = 1/2 (v/v).

(EC)-based electrolytes with a melting point of 37 °C. If PC, which has a melting point of −49 °C, can be used to form a rigid SEI and suppress coinsertion in the first cycle, the choice of the main solvent for the electrolyte will be expanded and battery performance will be improved. Such a search was conducted by the group of C. Wan and M. Yoshio et al. They found that the use of 1,3-benzodioxol-2-one ($C_6H_4CO_3$) as an additive significantly suppressed the degradation of PC molecules on graphite anodes during lithium insertion in the first cycle [6]. The group of G. H. Wrodnigg, J. O. Besenhard, and M. Winter et al. also found that the addition of 5 vol % ethylene sulfite (ES) to an electrolyte containing PC as the solvent suppressed the co-intercalation of PC into graphite and resulted in superior low-temperature performance compared to

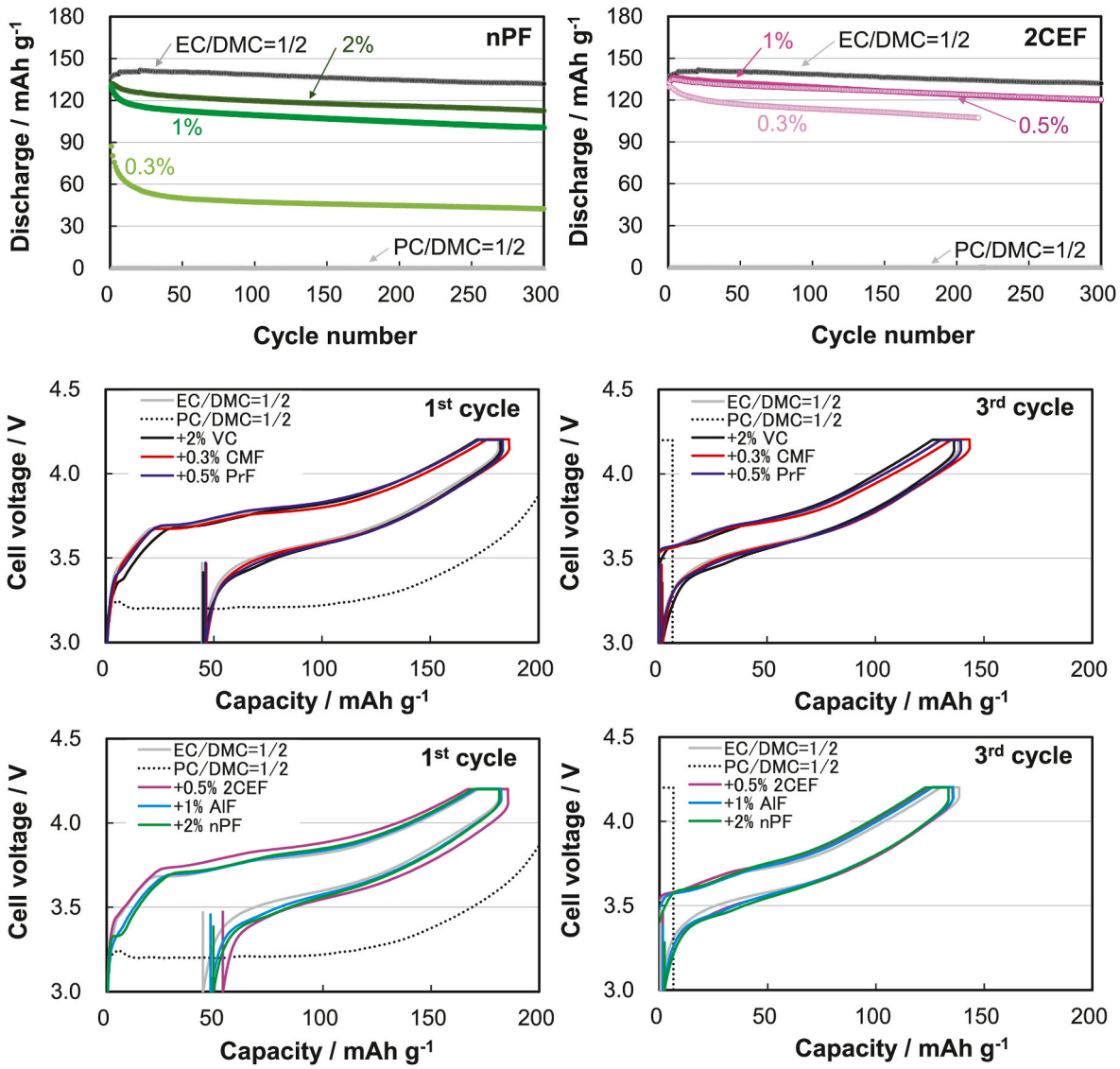

Fig. 2. (*continued*).

EC/DMC [7].

Since then, electrolyte research had shifted away from naturally-forming SEIs and toward intentionally trying to control the SEIs with additives. Especially, since 1999, when we proposed the concept of "functional electrolytes" in which a small amount of additive in the electrolyte is intentionally allowed to decompose before the main solvent decomposes to control the electrode interface [8,9], interest in additives that most economically and effectively improve the LIB performance had dramatically increased [10–14]. Since then, remarkable technological progress has led to additives with various functions, including not only anode additives, but also cathode additives, overcharge protection additives, corrosion prevention additives, impedance reduction additives, wettability improvement additives, and others [11,12].

When using a graphite anode, the best known additive for anodes in the world is vinylene carbonate (VC, 1a). In 1994, B. Simon and J. Boeuve developed a LIB with a graphite anode, an electrolyte containing a small amount of VC with a reduction potential of more than 1 V (vs. Li/Li^+) in a high dielectric constant and low viscosity solvent [15]. In 1997, C. Jehoulet et al. found that VC as an additive in a propylene carbonate (PC) based electrolyte can also suppress gas generation [16]. In 2000, we found that when the organochlorine impurities of VC in the electrolyte were eliminated, the reductive decomposition potential of VC on the graphite anode changed to less than 1 V, showing an even better coulombic efficiency than before [17]. Since then, VC research has exploded.

Subsequently, we turned to additives that contain double bonds, such as vinyl acetate and vinyl adipate [18]. The additive with a vinyl group ($-CH{=}CH_2$) at the end of its structure was found to easily polymerize in the presence of the Lewis acid, $LiPF_6$, in the electrolyte, although it had a cycling performance equivalent to that of VC. When the vinyl group was changed to an allyl group ($-CH_2CH{=}CH_2$), polymerization did not occur, but the cycling performance was found to be inferior to that of the additive with a vinyl group. When the allyl group was changed to a triple bonded propargyl group ($-CH_2C{\equiv}CH$), the cycling performance was equal to or better than that of the vinyl group, and no polymerization also occurred [19,20]. More recently, several additives with $-C{\equiv}N$ or $-C{\equiv}CH$ groups have been found to have Al corrosion inhibiting effects [21]. Thus, triple bond compounds still have an unknown potential and are worthy of searching for new structures.

In contrast, compounds with formyl groups, while promising because of their low molecular weights, have been avoided in research because they are prone to corrosion and are easily oxidized or reduced. Accordingly, we were interested in whether corrosion could be inhibited

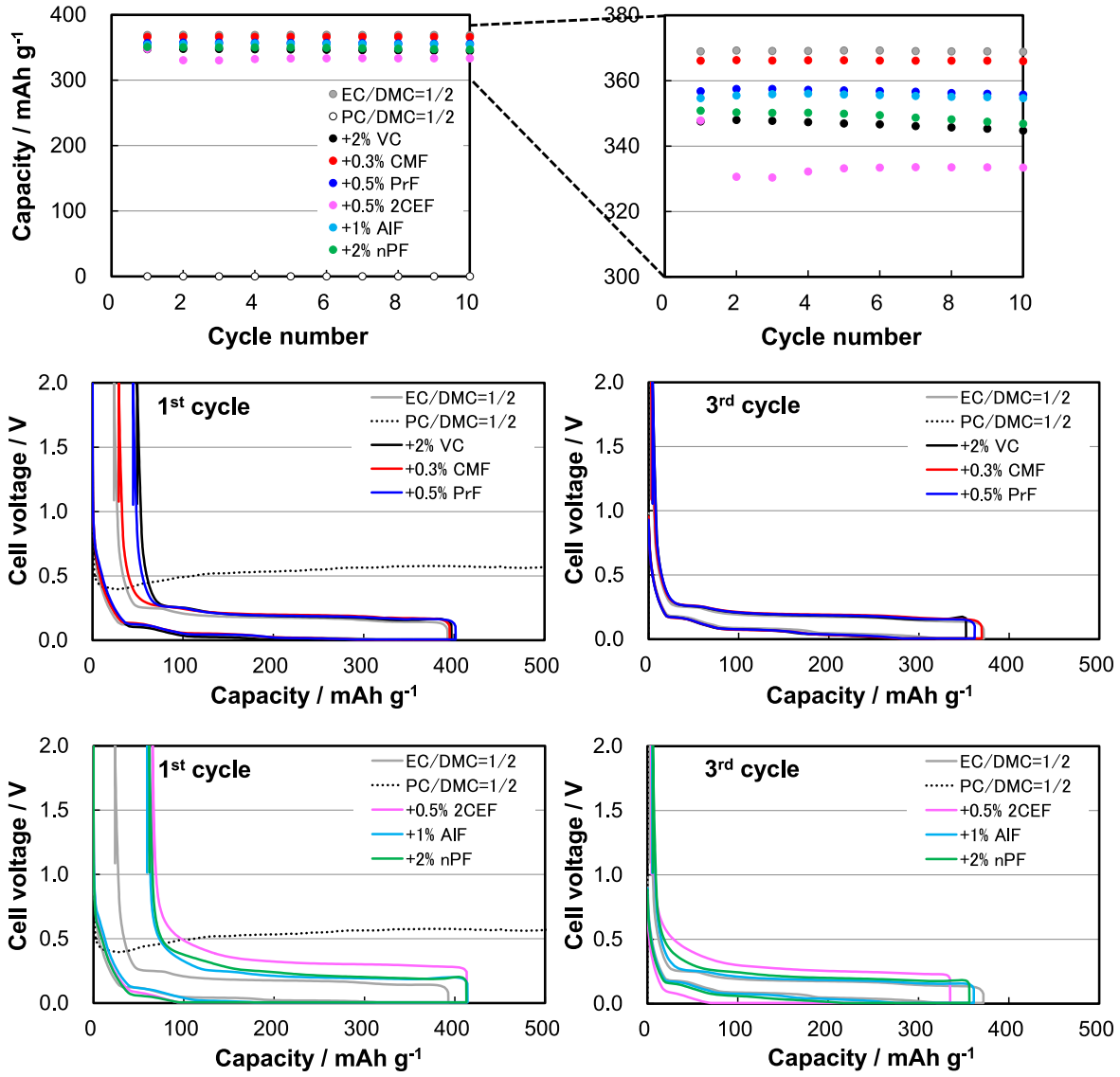

Fig. 3. NG/Li and NCM523/Li half-cell 1C rate charge-discharge curves and cycling performance with 1M $LiPF_6$ PC/DMC = 1/2 (v/v) + additive, reference is 1M $LiPF_6$ EC/DMC = 1/2 (v/v).

by combining the -C≡N and propargyl groups, which have corrosion-inhibiting effects, with formyl groups, which easily corrode. Also, since electrochemical decomposition of the additives occurs in "moles", the higher the molecular weight, the higher the weight ratio of the additive in the electrolyte. In other words, the lower molecular weight means that the amount of the additive weight ratio can be reduced. Another way to look at it, a simple structure has the advantage of having no unnecessary parts that can break down electrochemically and degrade battery performance. This will reduce the risk of liquid depletion in high-capacity batteries, where there is little space for the electrolyte to enter. The group of J.-Y. Eom et al. reported that the VC remaining after SEI formation decomposes on the cathode side [22]. For these reasons, we decided to challenge the possibility that formyl esters containing triple bonds do not promote corrosion, that extra additives do not decompose on the cathode, and that small additions minimize weight loss in the electrolyte.

2. Experimental

2.1. Chemicals

Cyanomethyl formate (CMF), n-propyl formate (nPF), succinonitrile (SN), adiponitrile, 1,5-hexadiyne, 1,5-hexadiene, and hexane were purchased from Tokyo Chemical Industry (TCI) Co., Ltd. Propargyl formate (PrF) and allyl formate (AlF) were synthesized according to the method of J. Deutsch and H. J. Niclas [23]. 2-Cyanoethyl formate (2CEF) was synthesized by a common method. They were used without further purification and stored over 4 A molecular sieves. Battery grade vinylene carbonate (VC), controlled to H_2O: <10 ppm, was purchased from the MU Ionic Solutions Corporation, battery grade controlled to H_2O: <10 ppm. 1M $LiPF_6$ PC/DMC = 1/2 (v/v) and 1M $LiPF_6$ EC/DMC = 1/2 (v/v) electrolytes, controlled to H_2O: <10 ppm and HF: <30 ppm, were also purchased from the MU Ionic Solutions Corporation.

2.1.1. Synthesis of propargyl formate (PrF)

To synthesize PrF, potassium formate (154 g, 1.84 mol) was suspended in anhydrous sulfolane (115 ml) and ethyl methyl carbonate

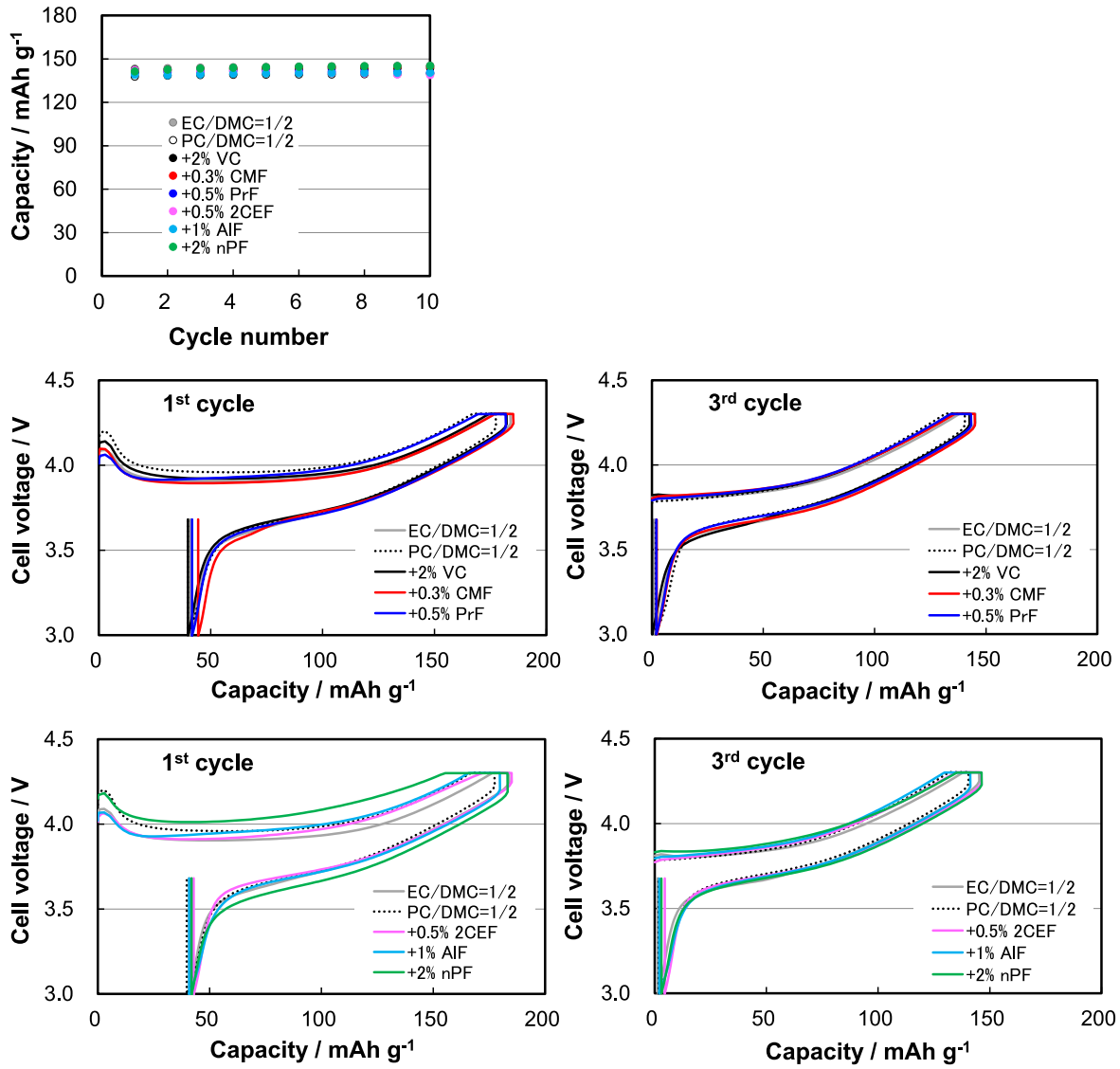

Fig. 3. (*continued*).

(230 ml) at 25 °C. To this suspension was added propargyl chloride (94.5 g, 1.23 mol) and potassium iodide (7.7 g, 0.044 mol). The reaction mixture was then heated at 100 °C for 3 h. After cooling to room temperature, the formed potassium chloride was filtered and washed twice with acetone. After distillation of the ethyl methyl carbonate, the product was next distilled under reduced pressure to yield 51.6 g (Yield: 49.4 %) of PrF at 62–67 °C/1.5 kPa. After distillation, these compounds were stored over 4 A molecular Sieves with H_2O: <10 ppm. The gas chromatograph (GC) analysis of the PrF synthesized in our laboratory resulted in 99.1 % purity.

2.1.2. Synthesis of allyl formate (AlF)

To synthesize AlF, potassium formate (41.0 g, 0.487 mol) was suspended in anhydrous sulfolane (156 ml) at 25 °C. To this suspension was added allyl chloride (25.2 g, 0.329 mol) and potassium iodide (2.10g, 0.026 mol). The reaction mixture was then heated at 77 °C for 5.5 h. After cooling to room temperature, the formed potassium chloride was filtered and washed twice with sulfolane. The product was next distilled under reduced pressure to yield 5.16 g (Yield: 18.2 %) of AlF at 24–29 °C/5.0 kPa. After distillation, these compounds were stored over 4 A molecular Sieves with H_2O: <10 ppm. For AlF the synthesized in our laboratory, the GC purity result was 99.9 %.

2.1.3. Synthesis of 2-cyanoethyl formate (2CEF)

To synthesize 2CEF, 117 g (1.60 mol) of ethylene cyanohydrin was added to 150 g (3.20 mol) of 98 % formic acid, then refluxed for 2 h under Ar. The product was next distilled under reduced pressure to yield 88.5 g (Yield: 55.9 %) of 2CEF at 89 °C/57.5 kPa. After distillation, these compounds were stored over 4 A molecular Sieves with H_2O: <10 ppm. For the 2CEF synthesized in our laboratory, the GC purity result was 97.2 %.

2.2. 2032-coin cells evaluation

2032-coin cells (charge capacity: 2.3 mAh) were used for the charge/discharge tests. The coin cell experimental method is based on our previously reported work [24]. All the electrode sheets were purchased from The Furukawa Battery Co., Ltd. For the full-cell, the composition of the cathode sheet was $LiNi_{0.5}Co_{0.2}Mn_{0.3}O_2$ (NCM523)/acetylene black (AB)/polyvinylidene fluoride (PVdF) = 92/5/3, Ø14 mm coated on aluminum foil. The anode sheet was natural graphite (NG)/styrene butadiene rubber (SBR)/carboxymethyl cellulose (CMC) = 98/1/1, Ø15 mm coated on copper foil. In this paper, the positive electrode will be referred to as the cathode and the negative electrode as the anode. The N/P ratio in all the cells was approximately 1.3. Between the electrodes,

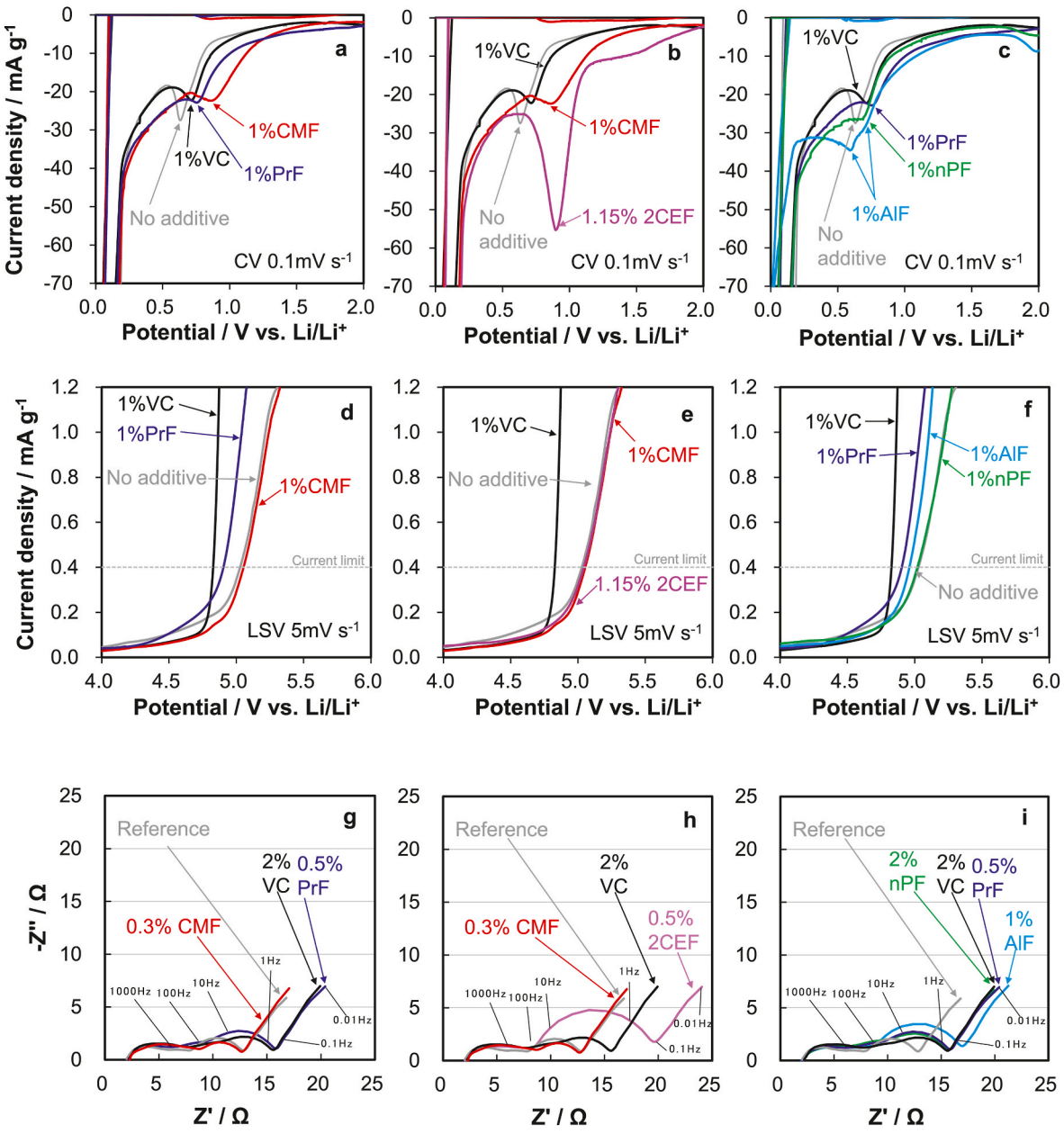

Fig. 4. Cyclic voltammetry measurement (a–c) of NG/Li/Li three-electrode glass cell, 0.1 mV s^{-1} (1^{st} cycles) and linear sweep voltammetry (d–f), AB/Li/Li three-electrode glass cell, 5 mV s^{-1} measurement for additives in 1M $LiPF_6$ EC/DMC = 1/2 (v/v). g-i are full-cell impedance measurements at 50% SOC state (21^{st} cycle) with 1M $LiPF_6$ PC/DMC = 1/2 (v/v) + additive, reference is 1M $LiPF_6$ EC/DMC = 1/2 (v/v).

a 20 μm thick triple-layer PP/PE/PP separator (Ube Maxell) and glass fiber filter paper GF/A (Whatman) were used. The Ø19 mm separator was placed toward the NG anode and the Ø16 mm glass fiber filter toward the NCM523 cathode.

The NG/Li half-cell used a Ø15 mm anode electrode and a Ø14 mm, 0.25 mm thick Li metal foil mounted on a Ø15 mm stainless steel grid (100 mesh). A 20 μm thick 3-layer PP/PE/PP separator was placed at Ø19 mm facing the NG anode and a glass fiber filter paper GF/A at Ø16 mm facing the Li foil. In another NCM523/Li half-cell, a Ø15 mm anode electrode was replaced by a Ø14 mm cathode electrode. The electrolytes used were 1M $LiPF_6$ PC/DMC = 1/2 (v/v) and 1M $LiPF_6$ EC/DMC = 1/2 (v/v). Approximately 0.2 cm^3 of electrolyte was injected into each coin cell.

The charging/discharging unit was an ACD-M01A (Aska Electronics) and all tests were conducted at 25 °C. The charge-discharge conditions for the NCM/NG full-cell were performed at 4.2 V-cccv to 3.0 V-cc and 1C rate (=2.3 mA). The charge-discharge conditions for the NG/Li half-cells were performed at 0.005 V-cccv to 2.0 V-cc and 0.61C rate (=2.3 mA), and for the NCM523/Li half-cells at 4.3 V-cccv to 3.0 V- cc and 1C rate (=2.3 mA).

2.3. Coin cell impedance

After 20 cycles, the coin cells from section 2.2 were charged 50 % (SOC = 50 %) and impedance was measured using a SP-150 potentiostat (Biologic Science Instruments) at 10 mV amplitude, 500 kHz-10 mHz at 25 °C.

2.4. Reductive decomposition potential

Cyclic voltammetry (CV) experiments were carried out using an NG/Li/Li (w/c/r) three-electrode glass cell at 25 °C. The working electrode

Table 1
Summary of the reductive, oxidative decomposition potentials and cell impedances.

Abbreviation	Additives	Dec. potential (V vs. Li/Li^+)		1M $LiPF_6$ PC/DMC=1/2 (v/v) NCM523/NG full cells		
		Red.	Ox.	5^{th} Disch. (mAh g^{-1}) (wt%)	$20^{th}/5^{th}$ (%)	21^{st} 50% SOC (Ω)
With -C≡N group						
CMF	Cyanomethyl formate	0.88	5.05	143 (0.3)	100.2	12.8
2CEF	2-Cyanoethyl formate	0.90	5.04	135 (0.5)	98.3	19.7
With -C≡CH group						
PrF	Propargyl formate	0.76	4.90	138 (0.5)	99.8	15.9
With -CH=CH_2 group						
AlF	Allyl formate	0.69	4.96	134 (1.0)	97.4	17.0
With -CH_2-CH_3 group						
nPF	n-Propyl Formate	0.65	5.02	130 (2.0)	96.7	15.7
References						
VC	Vinylene carbonate	0.72	4.83	133 (2.0)	97.3	15.6
1M $LiPF_6$ EC/DMC=1/2(v/v)		0.63	5.03	139	101.2	12.9

of the three-electrode glass cell was a stainless steel grid welded to a stainless steel plate. The graphite on the anode sheet described in section 2.2 was then pressed onto this stainless steel grid. The device was a SP-150 potentiostat (Biologic Science Instruments), and the measurement conditions were a potential range of 2.0 to 0.005 V at a scanning speed of 0.1 mV s^{-1}.

2.5. Oxidative decomposition potential

Linear sweep voltammetry (LSV) experiments were carried out using an AB/Li/Li (w/c/r) three-electrode glass cell at 25 °C. LSV was from open circuit voltage until the current reached 100 mA (cut off) at the scanning rate of 5 mV s^{-1} using a SP-150 potentiostat (Biologic Science Instruments). The oxidative decomposition potentials values were the potentials when the current density reached 0.4 mA g^{-1}. In the common NCM523 cathode electrode, carbon is used as a conductivity enhancer. To represent the real decomposition, we used an acetylene black (AB) electrode as the working electrode for our oxidative decomposition potential measurements. The electrode was prepared by mixing AB (AB Li-400, Denka Black) with a 5 % PVdF solution in N-methyl-2-pyrrolidone (NMP) (#9305, Kureha Corporation) at the mass ratio of AB: PVdF = 70 : 30. The slurry was coated on Al foil, dried at 70 °C, roll pressed and welded to a 0.5 mm thick Al plate to form the AB electrode. (AB + PVdF was about 0.59 mg cm^{-2} = 0.41 mg AB cm^{-2}).

2.6. Graphite surface analysis

The anode samples used for the analysis were first disassembled after the fifth discharge of the full-cell and the anode sheet was removed. Next, they were washed three times with DMC to remove any residual electrolyte, dried, then measured. Scanning electron microscopy (SEM) was performed using a JSM-7001F from JEOL, and X-ray photoelectron spectroscopy (XPS) was performed using a ULVAC-PHI ESCA 5600.

The SEI thickness was measured by XPS. The SEI thickness was defined as the depth at which the concentration of carbon atoms, excluding Li atoms, reached 95 % of the total. Since the anode surface is not flat, it is very difficult to uniformly etch the surface. Therefore, the rate of change in the carbon concentration decreases near the boundary between the SEI and the anode. This is the reason why 95 % was defined as the threshold value for the boundary between the SEI and the anode.

2.7. GC analysis of the electrolyte after cycling

For the GC analysis of the electrolyte after cycling, the amount of added formate ester was unified to 2 wt% to increase the detection sensitivity. Otherwise, 20 cycles were performed under the same conditions as for the full cell in section 2.2. The electrolyte was removed from the disassembled full cell and the electrode sheet was washed three times with DMC to adjust the final solution to approximately 0.8 cm^3. GC was performed using a GC-2014 (FID) from Shimadzu. The analytical conditions were as follows: capillary column DB-1701 (30 m) (Agilent Technologies), injection temperature: 250 °C, detection temperature: 230 °C, column temperature increased from 50 °C (held for 5 min) to 180 °C at 10 °C/min and held at 180 °C for 12 min.

3. Results and discussion

3.1. Selection of additive

This research is the first investigation of cyanomethyl formate with a -$CH_2C{\equiv}N$ group that has a molecular weight equivalent to the world's best-known VC. The tested formate esters were cyanomethyl formate (CMF, Fig. 1b), propargyl formate (PrF, Fig. 1c), 2-cyanoethyl formate (2CEF, Fig. 1d), allyl formate (AlF, Fig. 1e), and n-propyl formate (nPF, Fig. 1f).

3.2. Charge/discharge cycling of NCM523/NG full-cell

The full cell cycling performance was investigated by adding CMF or PrF to the 1M $LiPF_6$ PC/DMC = 1/2 (PC based electrolyte) (Fig. 2). Naturally, the electrolyte without additives had a zero capacity. The best cycling performance was obtained with CMF at 0.3 wt%. Compared to the optimum amount of 2 wt% for VC, CMF could be added at the lowest amount.

Next, PC-based electrolytes with 2CEF, which has a structure similar to CMF, and AlF and nPF, which are similar in structure to PrF, were also tested (top of Fig. 2). The results showed that the optimum addition amount of 2CEF (-$CH_2CH_2C{\equiv}N$), in which one CH_2 of CMF (-$CH_2C{\equiv}N$) was extended, required two times higher amount than that of CMF. This result was similar to the trend in our previous paper that showed that a conversion of vinyl groups to allyl groups reduced the cycling performance [18]. AlF, in which the -$CH_2CH{\equiv}CH$ group of PrF was replaced by the -$CH_2CH{=}CH_2$ group, also showed a three times higher the amount than that of CMF and two times higher than that of PrF (-$CH_2C{\equiv}CH$). This result was similar to the trend in our previous paper that compared methyl propargyl carbonate to allyl methyl carbonate or propargyl methanesulfonate to allyl methanesulfonate [19]. The nPF with the -$CH_2C{\equiv}CH$ group in PrF and the -$CH_2CH{=}CH_2$ group in AlF replaced by a single bond, required seven times the amount of additives compared to CMF and also had a poor cycling performance. If the SEI layer is fragile, the surface of the graphite anode will react with the PC-based electrolyte, causing a reduced battery capacity. However, the electrolyte containing formate esters in this work exhibited a good cycling performance of over 300 cycles, suggesting that the SEI layer was rigid and tough.

The voltage profile also showed that PC/DMC = 1/2 + no additives kept the decomposition current flowing (bottom of Fig. 2). The irreversible capacity and polarization of PC/DMC = 1/2 + 0.3 wt% CMF, PC/DMC = 1/2 + 0.5 wt% PrF and PC/DMC = 1/2 + 2 wt% VC in the first cycle were very similar, and the third cycle polarization of only PC/DMC = 1/2 + 0.3 wt% CMF was slightly better than the others. However, since the additives are reductively decomposed around 3.3 V in the first cycle, the voltage graphs for VC, AlF, and nPF above 1 wt% addition have a clear discrepancy to around 3.7 V compared to no EC/DMC + addition. These results indicated that the choice of the substituent connected to the formyl group has a significant impact on the cycling

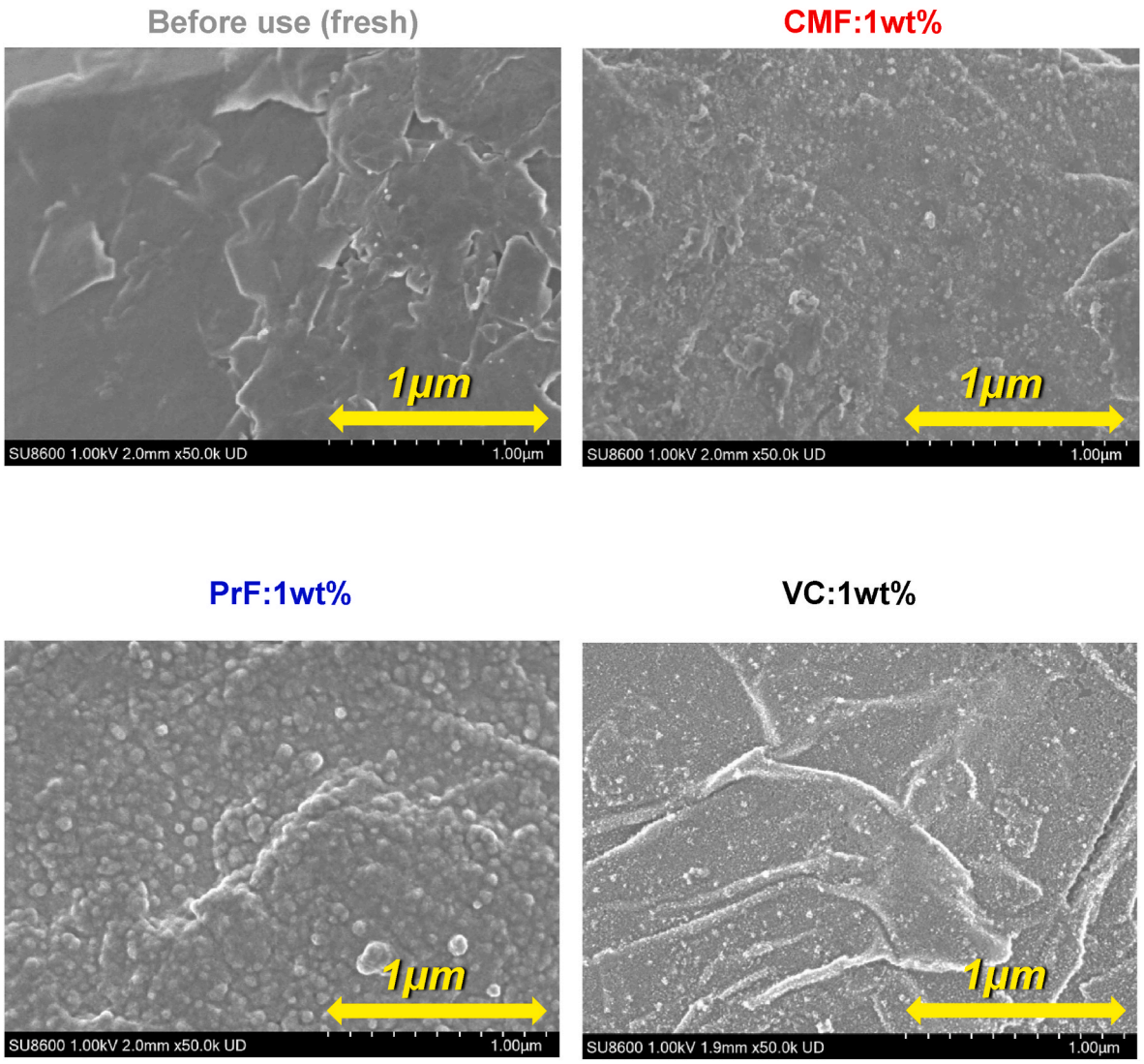

Fig. 5. SEM images, XPS depth profile measurements and XPS measurements of the graphite anode surface at the 5th discharge with [1M $LiPF_6$ EC/DMC = 1/2 (v/v)] + additives.

performance, and that the SEI-forming additives are preferable in smaller amounts. It is suggested that formate esters with -$CH_2C{\equiv}N$ or -$CH_2C{\equiv}CH$ groups, which can be added at a lower amount, have the advantage of a thinner SEI and higher Li-ion permeability.

3.3. Notes on additive synthesis

There is a point to be noted in the synthesis of PrF and AlF. When formic acid and an alcohol are used as the raw materials, the boiling points of the raw materials, the products, and the water by-product of the reaction are all near 100 °C. Moreover, the products were quite soluble in water, making it difficult to purify them to more than 90 %. Therefore, we changed the process to one that does not generate water by using potassium formate and organic chlorides as the raw materials, and found that PrF and AlF could be synthesized with a high purity and good yield [24]. On the other hand, 2CEF was synthesized using formic acid and an alcohol as the raw materials because the boiling point of 2CEF is high (over 200 °C) and almost insoluble in water, making it easy to separate both the raw materials and water.

3.4. Charge/discharge cycling of NG/Li half-cell

To clarify whether the addition effect was cathode- or anode-derived, it was evaluated in NG/Li half-cells (top of Fig. 3). The results showed a very high correlation to the graphite anodes. Regarding the cycling performance of the NG/Li half-cell, PC/DMC = 1/2 + no additive was 0 mAh g^{-1}, similar to the full-cell results. This confirmed that additives forming an SEI are essential for PC-based electrolytes. Although it did not reach the theoretical capacity of 372 mAh g^{-1} for graphite because these were done at the 0.61C rate, only PC/DMC = 1/2 + 0.3 wt% CMF (366 mAh g^{-1}) showed a capacity comparable to EC/DMC = 1/2 (369 mAh g^{-1}). The results of using other additives were clearly lower than the theoretical capacity of graphite of 372 mAh g^{-1}, with PC/DMC = 1/2 + 0.5 wt% PrF (356 mAh g^{-1}) and PC/DMC = 1/2 + 1 wt% AlF (355 mAh g^{-1}) in the order of highest tenth cycle capacity being almost equal. The PC/DMC = 1/2 + 2 wt% nPF (347 mAh g^{-1}) and PC/DMC = 1/2 + 2 wt% VC (345 mAh g^{-1}) were nearly equivalent. The lowest capacity was PC/DMC = 1/2 + 0.5 wt% 2CEF (333 mAh g^{-1}). This confirmed that CMF with the -$CH_2C{\equiv}N$ group on the HCOO group was specific.

The voltage profile of the NG/Li half-cell, PC/DMC = 1/2 + no additive, kept the decomposition current flowing all the time. Only the irreversible capacity and polarization of PC/DMC = 1/2 + 0.3 wt% CMF

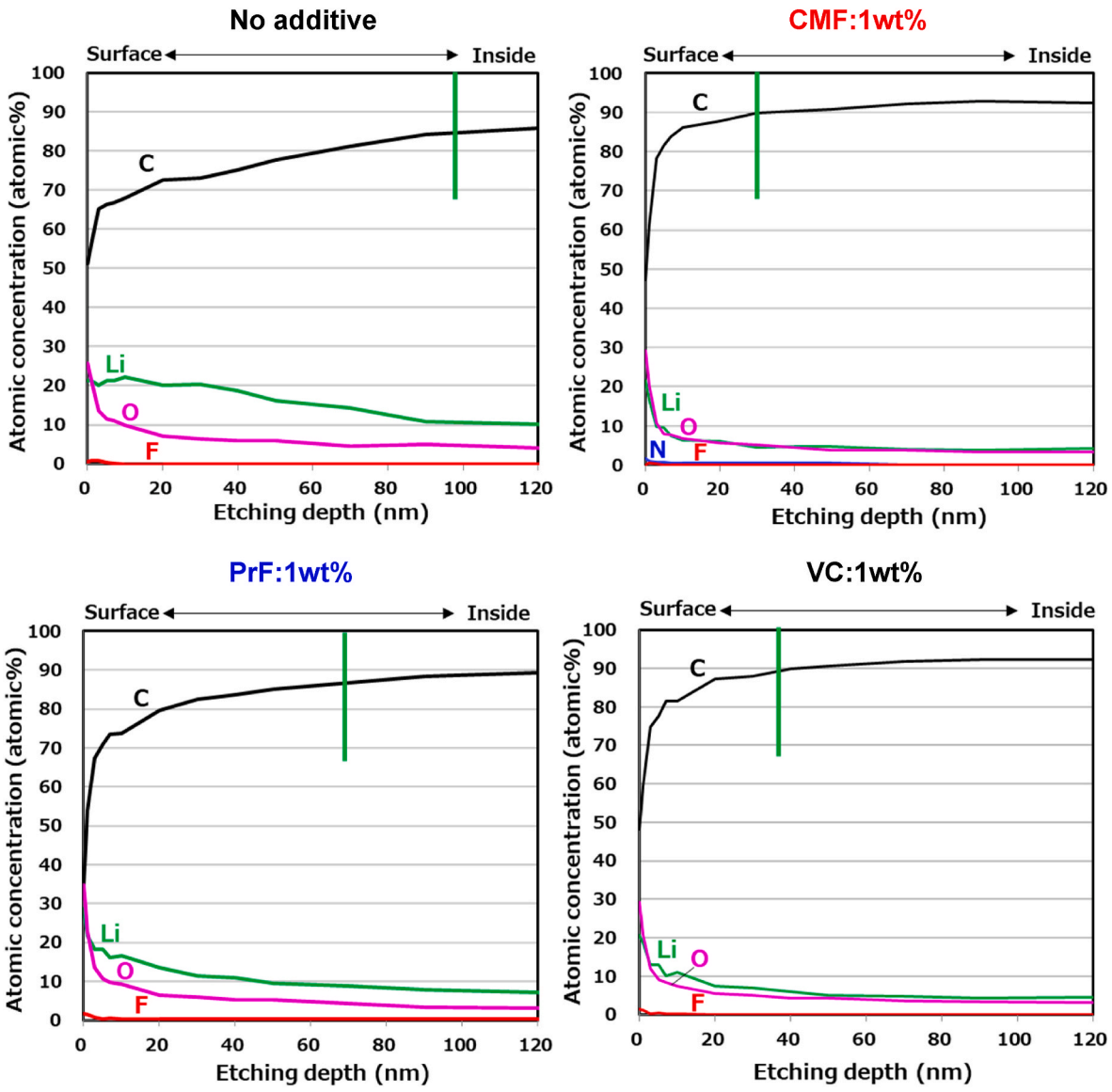

Fig. 5. (*continued*).

were very similar to those of EC/DMC = 1/2. The irreversible capacity and polarization of PC/DMC = 1/2 + 0.5 wt% PrF were very similar to those of PC/DMC = 1/2 + 2 wt% VC. On the other hand, the irreversible capacity and polarization of PC/DMC = 1/2 + 1 wt% AlF, PC/DMC = 1/2 + 2 wt% nPF, and PC/DMC = 1/2 + 0.5 wt% 2CEF were higher than those of EC/DMC = 1/2 and PC/DMC = 1/2 + 2 wt% VC. Again, this confirmed that CMF has a better ability to form the SEI than VC.

3.5. Charge/discharge cycling of NCM523/Li half-cell

In contrast, the capacity of the NCM523/Li half-cells at the 1C rate were almost equal and not significantly different (bottom of Fig. 3). The voltage profile of the NCM523/Li half-cell also showed that only PC/DMC = 1/2 + 0.3 wt% CMF was very similar in irreversible capacity and polarization to EC/DMC = 1/2 and PC/DMC = 1/2 + 2 wt% VC. The irreversible capacity and polarization of PC/DMC = 1/2 + 0.5 wt% PrF were very similar to those of PC/DMC = 1/2. The others, PC/DMC = 1/2 + 1 wt% AlF, PC/DMC = 1/2 + 2 wt% nPF, and PC/DMC = 1/2 + 0.5 wt % 2CEF, had a greater polarization than PC/DMC = 1/2 + 2 wt% VC. Since the formate esters are reduced and decomposed to the SEI on the anode side, it is unlikely that the CEI is formed on the cathode side.

3.6. Electrochemical evaluation

Furthermore, we investigated the reductive decomposition potential of the formate esters. Since the molecular weights of these additives are almost the same, we decided to set all the additive amounts to 1 wt%. The thresholds for the relative reduction decomposition potentials were compared at the peak top potentials.

The reductive decomposition potentials of the additives are shown higher than VC for CMF and close to VC for PrF (upper row of Fig. 4). This means that the reductive decomposition of CMF is before VC, indicating that it forms the SEI earlier the VC. When there is a CMF reductive decomposition peak, the 0.6 V EC reductive decomposition peak observed at EC/DMC = 1/2 + no additive disappears, indicating that the CMF inhibited the reductive decomposition of EC. In contrast, the reductive decomposition potential of PrF was very close to that of VC, indicating that it formed an SEI at the same time as VC. When there is a PrF reductive decomposition peak, it trails the 0.6 V EC reductive decomposition peak, indicating that PrF does not fully inhibit the reductive decomposition of EC. Although the reductive decomposition potentials of CMF and 2CEF are close, there is a significant difference in the amount of the 2CEF reductive decomposition compared to CMF. The

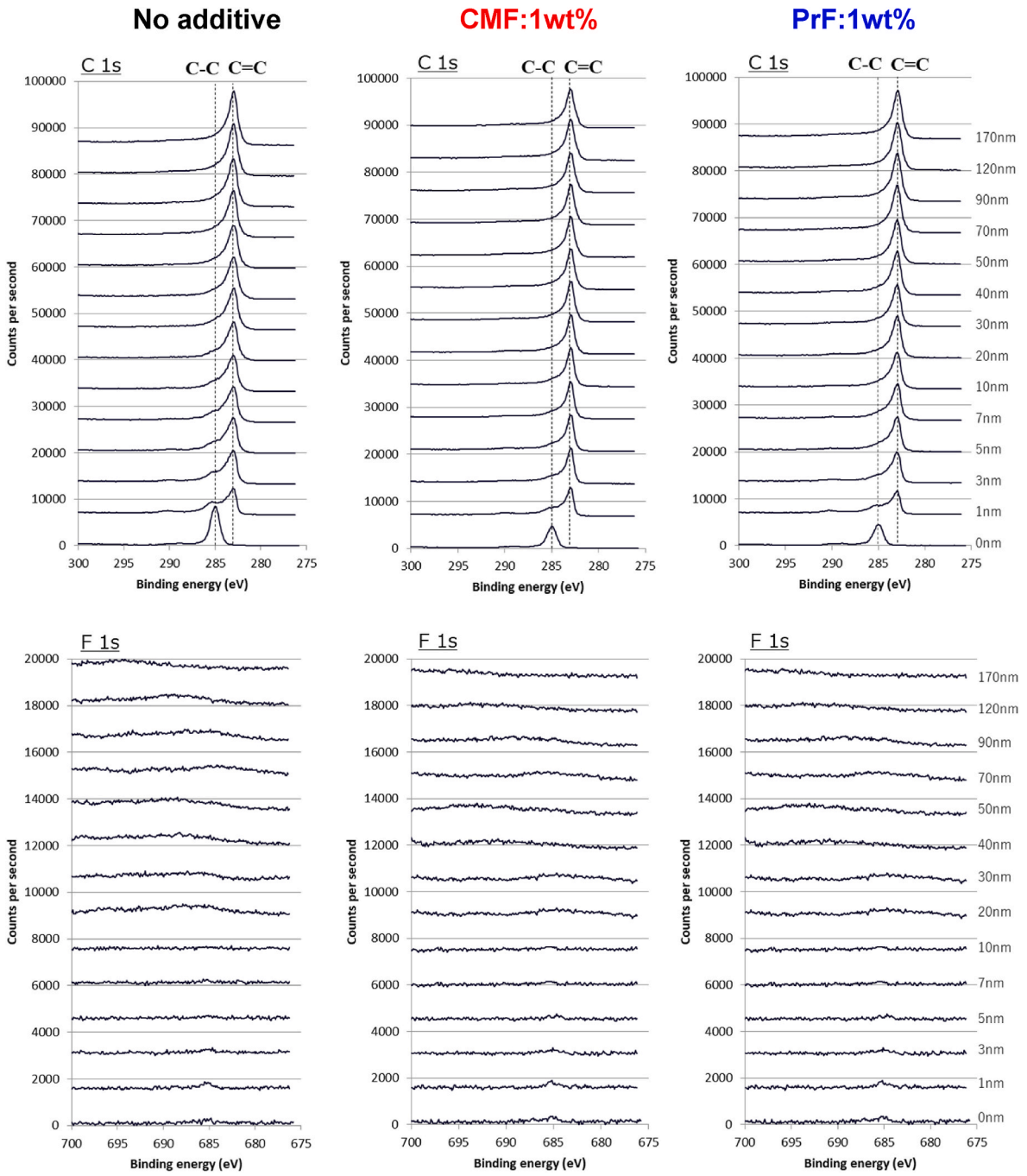

Fig. 5. (*continued*).

extremely high level of the 2CEF reductive decomposition compared to CMF suggests that the Li-ion permeability of the SEI reduced and decomposed on the surface of the graphite anode is also important. The reductive decomposition peaks of AlF and nPF also tailed the 0.6 V EC reductive decomposition peak, as did PrF and VC, indicating that the EC reductive decomposition cannot be completely inhibited. Based on this information, it is assumed that the difference in battery performance is due to the addition amount and the lithium-ion permeability of the SEI. In any case, only the reductive decomposition potential of CMF is higher, probably because electron-withdrawing groups, such as the -$CH_2C{\equiv}N$ groups, facilitate reductive decomposition.

On the other hand, the relative oxidative decomposition potentials were compared as a threshold value of 0.4 mA g^{-1}. The oxidation potentials of no additives, CMF, and 2CEF were comparable and clearly higher than the oxidation potential of VC (middle row of Fig. 4). The other oxidation potentials showed that single bonded nPF, double bonded AlF, and triple bonded PrF, in that order, were also higher than VC. Thus, it was clear that all the formate esters in this research were found to be less susceptible to oxidative decomposition at the cathode than VC.

Finally, the cell impedance was evaluated by adding the minimum optimum quantity of these formate esters (bottom row of Fig. 4). Since the reductive decomposition of CMF occurs at a time prior to that of VC, the increase in cell impedance could be suppressed with a smaller added amount of CMF than that of VC. This may be due to the fact that a thin SEI with a high Li-ion permeability can be obtained by adding a small amount. In contrast, the cell impedance of 2CEF was the highest of the formate esters investigated in this research. The reason for this is

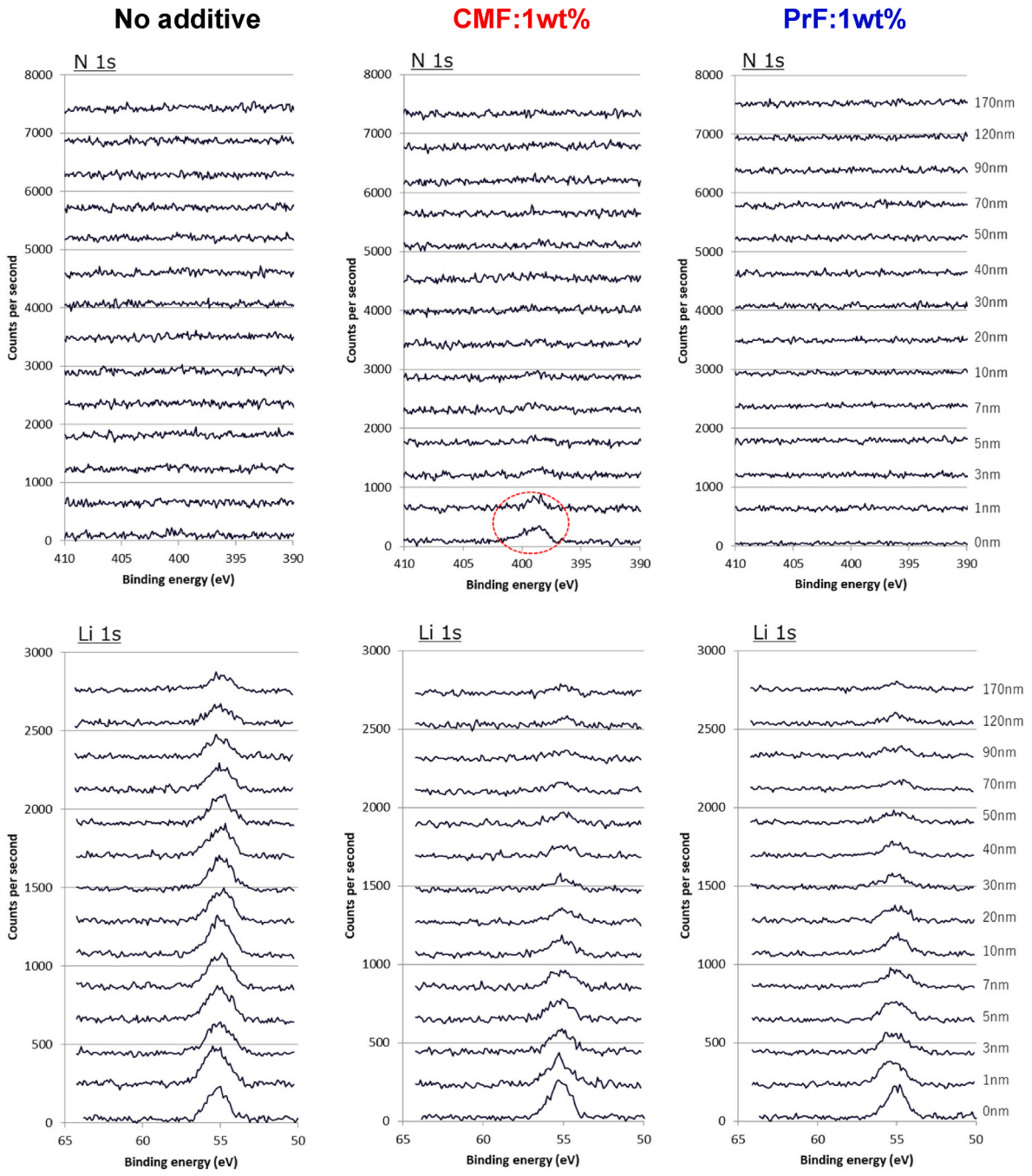

Fig. 5. (*continued*).

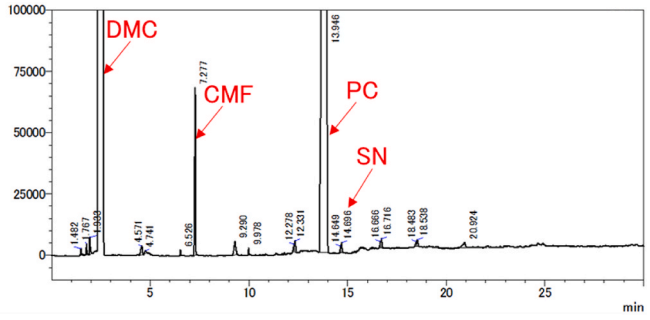

Fig. 6. GC analysis of PC-based electrolyte with CMF in full-cell after 20 cycles.

inferred to be that the amount of the reductive decomposition is extremely higher than that of the CMF, resulting in a high 2CEF reductive decomposition and thickening of the SEI. PrF, AlF, and nPF showed a reductive decomposition potential similar to that of VC, and their cell impedance was also comparable to that of VC. The amount of added PrF is slightly more than that of CMF, but less than that of VC, suggesting that PrF also forms a relatively thin SEI.

Lastly, no Al corrosion was visually observed. In addition, there was no sudden drop in capacity during the cycling, it is presumed that the metal corrosion that had been a concern did not occur.

A summary of the results of the study is given in Table 1.

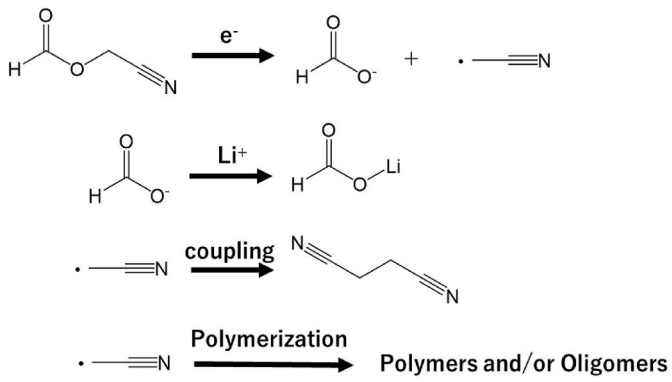

Scheme 1. Proposed mechanism of CMF decomposition occurring in graphite anode.

3.7. SEI analysis

Based on the results of the electrochemical evaluation, the SEM and XPS of the anode surfaces were compared focusing on CMF and PrF. SEM measurements observed that CMF and PrF formed a slightly rougher membranes than VC (Fig. 5). The top left SEM image shows a typical graphite electrode before starting the electrochemical experiments. As can be seen from the images of CMF, PrF, and VC, the additives prevented graphite exfoliation and produced a uniform SEI layer on the graphite. Furthermore, the surface morphology on CMF, which showed the best performance in terms of cycling performance, was found to be relatively similar to that of VC. In contrast, the surface morphology of PrF was more granular and clearly different from that of CMF. The PrF results are similar to the SEM images of methanesulfonylpropargyl (PMS) with propargyl groups reported in our previous paper, which may be a surface state specific to propargyl groups [18].

Following the SEM images, the depth distribution of the SEI was measured using XPS (Fig. 5). Although the measured SEI thickness may not be absolute, since the goal is to compare the relative SEI thickness between additives, the thickness definition described in section **2.6** was used. In the case of CMF, the SEI was the thinnest with a thickness of approx. 30 nm, and the impedance was the lowest. In the case of VC, the SEI thickness was approx. 40 nm and the impedance was also slightly higher than that of CMF. In the case of PrF, the SEI thickness was thicker than that of VC, approx. 70 nm, but the impedance was similar to that of VC. The SEI thickness of 1M $LiPF_6$ EC/DMC = 1/2 (v/v) + no additive was the largest, approx. 100 nm, but the impedance was comparable to VC. These results suggest that the SEI of CMF is denser than that of VC and easily permeable to Li ions. Therefore, it is considered that PC intercalation was suppressed and a good cycling performance was achieved.

The anode surface was analyzed by XPS measurements. The XPS data for Li1s, F1s, C1s, and N1s are shown in Fig. 5. No significant difference was observed in the C1s spectra of CMF and PrF compared to no additive. It was hypothesized that the formate esters containing triple bonds were polymerized after reductive decomposition. However, the lack of significant changes in the C-C and C-H bond strengths did not allow a clear elucidation of the polymer hydrocarbon species and bonding states derived from the unsaturated bonds. No significant difference was observed in the F1s spectra of CMF and PrF compared to no additive. Thus, it was suggested that the amount of the inorganic membrane, such as $LiPO_2F_2$ (687 ev) and LiF (685 ev) containing F, is almost the same. On the other hand, the N1s spectra showed C≡N-like species in the shallow part only for CMF, suggesting that -C≡N groups are present in the surface layer. The Li1s spectra of CMF and PrF show that the ratio of Li present in the depth profile is in the order of CMF < PrF < no additive, which is consistent with the aforementioned trend of the depth distribution of the SEI. This is thought to be due to the fact that CMF and PrF suppress Li consumed by the SEI and the Li-containing organic membrane formed on the graphite surface is thinner, thereby increasing the Li-ion permeability. Based on the above SEI analysis, it is clear that battery performance is significantly affected by the thickness and quality of the SEI, which is determined by the additive structure.

3.8. Electrolyte analysis

Since we could not obtain sufficient evidence of the mechanism from the XPS, we removed the electrolyte from the dismantled battery and used GC to directly obtain information on the decomposition products of the additives. When CMF was used as an additive, a small succinonitrile (N≡C-CH_2CH_2-C≡N, SN) peak was qualitatively detected (Fig. 6). Identification of SN was performed by overlaying with purchased reagents. There were several peaks other than SN, and it did not produce SN in a highly-selective manner. Other batteries with formate esters were similarly analyzed by GC. nPF detected a peak of hexane (H_3C-$(CH_2)_4$-CH_3), albeit in trace amounts. On the other hand, a peak of adiponitrile (N≡C-$CH_2CH_2CH_2CH_2$-C≡N) was not detected in 2CEF. 1,5-hexadiyne (HC≡C-$CH_2CH_2CH_2$-C≡CH) in PrF, and 1,5-hexadiene (H_2C=CH-CH_2CH_2-CH=CH_2) in AlF were also not detected.

The effect of using SN as an additive in NCM523/graphite batteries has already been reported by the group of H. Songyi et al. [25]. Under high voltage, pouch cells with 0.5 wt% SN are stated to have a significantly improved cycling stability and reduced impedance, as SN forms an electrode/electrolyte interface film on the cathode surface, suppressing the decomposition of the main solvent of the electrolyte and the elution of metal ions from the cathode.

The group of H. Ota et al. states that the VC-derived SEI layer is composed of polymer species such as poly (VC), oligomers of VC, ring-opened polymers of VC, and polyacetylene [26]. Presumably, formate esters are similarly formed by the one-electron reduction of radical products, transferring radicals between carbons to form various oligomers and polymers.

Based on the above results, the mechanism of SEI formation is proposed in Scheme 1. CMF may undergo an one-electron reduction on the graphite anode surface to the HCOO anion and CH_2C≡N radical. The HCOO anion would react with a Li ion to deposit insoluble HCOOLi on the anode surface, and the CH_2C≡N radical would undergo homocoupling to form SN. However, the active CH_2C≡N radical is prone to various side reactions, and SN was not produced in a highly-selective manner, thus it will be conceivable that various oligomers and polymers can be formed on the anode surface. Unfortunately, at this stage, there is insufficient direct evidence to support this argument, and further research is underway.

4. Conclusion

Critical battery performance, such as the capacity and voltage, is governed by the electrode active material, and the primary role of the electrolyte is how to control the electrode interface. Especially, our research is based on the idea that controlling the anode interface is an important factor in improving battery performance, such as cycling performances and suppression of increasing impedance.

As a result, we found that among the formate esters, CMF with the -CH_2C≡N group forms an excellent SEI as an electrolyte additive. The optimum addition amounts of CMF is 0.3 wt%, which is much lower than the optimum additive amount of 2 wt% for VC. Among others, CMF with the -CH_2C≡N group has a higher reductive decomposition potential than VC, a thinner SEI and a lower cell impedance due to the lower added amount, suggesting that CMF was a better Li-ion permeability. Furthermore, formate esters with the -C≡N groups do not cause corrosion and have a higher oxidative decomposition potential than that of VC, which holds promise for use in the high-voltage batteries.

Based on our results, there are two important points for the structural design of additives to control the SEI formation. One is the timing of the

SEI formation and the other is the quality of the SEI. Looking at CMF from that perspective, we were able to note that it has a high reduction decomposition potential, so the timing of the SEI formation is fast, and the low addition amount allows for a high quality SEI with a low impedance. The new knowledge obtained about the -$CH_2C{\equiv}N$ group is now expected to contribute to further improvement of the SEI-forming additives. It also suggests that CMF could replace VC as a practical electrolyte additive for high-voltage batteries in the near future.

CRediT authorship contribution statement

Koji Abe: Writing – review & editing, Writing – original draft, Supervision, Methodology, Investigation. **Masaki Deguchi:** Writing – review & editing, Writing – original draft, Data curation. **Yanko Marinov Todorov:** Writing – review & editing, Writing – original draft, Validation, Methodology, Data curation.

Declaration of competing interest

The authors declare the following financial interests/personal relationships that could be considered potential competing interests. Koji Abe and Yanko Marinov Todorov of Yamaguchi University sold patent publications number WO2023-219102 to Kyocera Corporation. The other author declare that he has no known competing financial interests or personal relationships that could affect the research reported in this paper.

Data availability

No data was used for the research described in the article.

References

[1] E. Peled, S. Menkin, J. Electrochem. Soc. 164 (2017) A1703, https://doi.org/10.1149/2.1441707jes.
[2] E. Peled, J. Electrochem. Soc. 126 (1979) 2047, https://doi.org/10.1149/1.2128859.
[3] E. Peled, *in* Lithium batteries, 1983th edition, J.-P. Gabano, Editors, Chapter 3, Lithium Stability and Film Formation in Organic and Inorganic Electrolyte for Lithium Battery Systems, p. 43, Academic Press, London.
[4] D. Aurbach, Y. Ein Ely, O. Chusid, Y. Carmeli, M. Babai, H. Yamin, J. Electrochem. Soc. 141 (1994) 603, https://doi.org/10.1149/1.2054777.
[5] J.O. Besenhard, M. Winter, j. Yang, W. Biberacher, J. Power Sources 54 (1995) 228, https://doi.org/10.1016/0378-7753(94)02073-C.
[6] C. Wang, H. Nakamura, H. Komatsu, M. Yoshio, H. Yoshitake, J. Power Sources 74 (1998) 142, https://doi.org/10.1016/S0378-7753(98)00017-2.
[7] G.H. Wrodnigg, J.O. Besenhard, M. Winter, J. Electrochem. Soc. 146 (1999) 470, https://doi.org/10.1149/1.1391630.
[8] H. Yoshitake, in: *Battery And Power Supply in Techno-Frontier Symposium*, Makuhari, Japan Management Associates, 1999. F5-3.
[9] K. Abe, H. Yoshitake, Electrochemistry 72 (2004) 520, https://doi.org/10.5796/electrochemistry.72.519.
[10] Sheng Shui Zhang, J. Power Sources 162 (2006) 1379, https://doi.org/10.1016/j.jpowsour.2006.07.074.
[11] H. Yoshitake, *in Lithium-Ion Batteries* (Modern Aspects of Electrochemistry, 58), 2009th Edition, M. Yoshio, R. J. Brodd, A. Kozawa, Editors, Chapter 19 Functional Electrolytes Specially Designed for Lithium-Ion Batteries, Springer, New York.https://doi.org/10.1007/978-0-387-34445-4_19.
[12] K. Abe, in *Electrolytes for Lithium and Lithium-ion Batteries* (Modern Aspects of Electrochemistry, 58), 2014th Edition, T. R. Jow, K. Xu, O. Borodin, and M. Ue, Editors, Chapter 3 Nonaqueous Electrolytes, and Advances in Additives, Springer, New York. https://doi.org/10.1007/978-1-4939-0302-3_3.
[13] A.M. Haregewoin, A.S. Wotango, Bing-Joe Hwang, Energy Environ. Sci. 9 (2014) 1955, https://doi.org/10.1039/C6EE00123H.
[14] Kang Xu, Chem. Rev. 114 (2014) 11503, https://doi.org/10.1021/cr500003w.
[15] B. Simon, J. Boeuve, US Patent 5, vol. 626, 1994, p. 981 (SAFT Romainville.): (1995) applied in 1994.
[16] C. Jehoulet, P. Biensan, J.M. Bodet, M. Broussely, C. Moteau, C. Tessier-Lescourret, Batteries for portable applications and electric vehicles, in: A.R. Landgrebe, C. F. Holmes (Eds.), The Electrochemical Society Proceedings Series, Pennington, NJ, 1997. PV 97-18, p. 974.
[17] T. Hamamoto, A. Ueki, K. Abe, T. Takai, US Patent 6,656,642, UBE Co., Ltd., 2003 applied in 2000.
[18] K. Abe, H. Yoshitake, T. Kitakura, T. Hattori, C. Wang, M. Yoshio, Electrochim. Acta 49 (2004) 4613, https://doi.org/10.1016/j.electacta.2004.05.016.
[19] K. Abe, T. Hattori, K. Kawabe, Y. Ushigoe, H. Yoshitake, J. Electrochem. Soc. 154 (2007) A810, https://doi.org/10.1149/1.2746570.
[20] K. Abe, K. Miyoshi, T. Hattori, Y. Ushigoe, H. Yoshitake, J. Power Sources 184 (2008) 449, https://doi.org/10.1016/j.jpowsour.2008.03.037.
[21] M. Deguchi, Y.M. Todorov, K. Abe, Electrochim. Acta 469 (2023) 143267, https://doi.org/10.1016/j.electacta.2023.143267.
[22] Ji-Yong Eom, In-Ho Jung, Lee Jong-Hoon, Power Sources 196 (Issue 22) (2011) 9810, https://doi.org/10.1016/j.jpowsour.2011.06.095.
[23] J. Deutsch, H.J. Niclas, Synth. Commun. 23 (11) (1993) 1561–1568, https://doi.org/10.1080/00397919308011251.
[24] M. Deguchi, D. Tazoe, Y.M. Todorov, K. Abe, J. Electrochem. Soc. 171 (2024) 040536, https://doi.org/10.1149/1945-7111/ad39cb.
[25] H. Songyi, L. Yan, Z. Hong, F. Chaojun, F. Weizhen, Yu Le, Du, Xueyong, Surf. Interface Anal. 52 (2020) 364–373, https://doi.org/10.1002/sia.6744.
[26] H. Ota, Y. Sakata, A. Inoue, S. Yamaguchi, J. Electrochem. Soc. 151 (2004) A1659, https://doi.org/10.1149/1.1785795.